EXPERIMENTAL AND THEORETICAL STUDY ON SPRAY BEHAVIORS OF MODIFIED BIO-ETHANOL FUEL EMPLOYING DIRECT INJECTION SYSTEM

by

Amirreza GHAHREMANI[a], Mohammad AHARI[b], Mojtaba JAFARI[b], Mohammad Hasan SAIDI[a*], Ahmad HAJINEZHAD[b], and Ali MOZAFARI[a]

Original scientific paper
DOI: 10.2298/TSCI160108253G

[a] Center of Excellence in Energy Conversion, School of Mechanical Engineering, Sharif University of Technology, Tehran, Iran
[b] Faculty of New Sciences and Technologies, University of Tehran, Tehran, Iran

One of the key solutions to improve engine performance and reduce exhaust emissions of internal combustion engines is direct injection of bio-fuels. A new modified bio-ethanol is produced to be substituted by fossil fuels in gasoline direct injection engines. The key advantages of modified bio-ethanol fuel as an alternative fuel are higher octane number and oxygen content, a long-chain hydrocarbon fuel, and lower emissions compared to fossil fuels. In the present study spray properties of a modified bio-ethanol and its atomization behaviors have been studied experimentally and theoretically. Based on atomization physics of droplets dimensional analysis has been performed to develop a new non-dimensional number namely atomization index. This number determines the atomization level of the spray. Applying quasi-steady jet theory, air entrainment and fuel-air mixing studies have been performed. The spray atomization behaviors such as atomization index number, Ohnesorge number, and Sauter mean diameter have been investigated employing atomization model. The influences of injection and ambient conditions on spray properties of different blends of modified bio-ethanol and gasoline fuels have been investigated performing high-speed visualization technique. Results indicate that decreasing the difference of injection and ambient pressures increases spray cone angle and projected area, and decreases spray tip penetration length. As expected, increasing injection pressure improves atomization behaviors of the spray. Increasing percentage of modified bio-ethanol in the blend, increases spray tip penetration and decreases the projected area as well.

Key words: *atomization index, bio-ethanol, visualization, spray characteristics*

Introduction

To reduce emissions and fuel consumption of spark ignition engines, employing bio-fuels in a direct injection (DI) engine is of interest in this research.

Wu *et al.* [1] examined the spray of oxygenate fuels such as dimethoxy methane, dimethyl carbonate, and dimethyl ether as an additive for engines by means of Mie scattering and particle image velocimetry techniques. Cone angle of oxygenate fuels were larger than that of diesel fuel while for the tip penetration the relationship was the opposite. Martin *et al.*

* Corresponding author, e-mail: saman@sharif.edu

[2] studied single and double injection of a gasoline DI piezo injector in a chamber. Their results verified that ambient pressure is more effective than ambient temperature on the spray behaviors. They also showed that spray tip penetration of the second injection was lower than that of the first injection as a result of increasing chamber pressure caused by first injection. Agarwal *et al.* [3] studied the effects of ambient pressure on the spray characteristics of Jatropha vegetable oil and Jatropha bio-diesel fuel and their blends in a visualized chamber. Based on their tests, decreasing the amount of the Jatropha in the blends reduces spray tip penetration, spray cone angle, and spray area of the injected fuel. Liu *et al.* [4] employing Schlieren technique in an optical combustion chamber investigated the spray evolution of compressed natural gas as an alternative fuel. Their results demonstrated that injection pressure has a significant influence on the spray tip penetration while ambient temperature has no important effect on the spray tip penetration and spray cone angle. Kumar and Kumar [5] compared spray tip penetration length of five different models by varying injection pressure. They chose Mahua oil as a bio-diesel fuel to analyze its characteristics. They found out that Hiroyasu's model [6] was the best model between all models studied in their research. Pan *et al.* [7] investigated spray and combustion characteristics of bio-diesel in a DI engine. They reported that using bio-diesel increases combustion duration and decreases ignition delay. Their results showed that increasing injection pressure increases spray tip penetration length and cone angle. Kim *et al.* [8] studied spray behavior and combustion properties of diesel and gasoline fuel in a DI engine. They used a constant volume chamber for non-evaporating condition and a visualized engine for evaporating situations. Their results demonstrated that spray tip penetration of gasoline and diesel fuel were similar for non-evaporating condition while gasoline had greater cone angle compared with diesel's. In evaporating condition both tip penetration and angle of diesel were larger than those of gasoline. They investigated flame properties, engine emission, and performance as well. Amount of produced CO, HC, and NO for gasoline fuel were higher than diesel's, although diesel fuel had created more soot formation compared with gasoline.

Lee and Park [9] employed phase Doppler particle analyzer and visualization to explore the influences of injection pressure on the atomization behavior and break up with the aid of multi hole gasoline DI. Their results revealed that injection pressure play an important role on the break-up phenomenon. They reported that increasing the injection pressure decreases Sauter mean diameter (SMD) till 20 MPa and after that increasing the injection pressure to 30 MPa has no important effect on SMD. Wu *et al.* [10] performing a high speed camera, visualized the lift-off flame of the injected spray in a controllable active thermo-atmosphere combustor and studied the spray and combustion properties of different blends of gasoline and diesel fuels. Kim *et al.* [11] studied the influences of injection strategies on spray characteristics, combustion, and emission in a premixed charge compression ignition engine. They also investigated the effects of adding ethanol to the diesel fuel on combustion and emission. Their results indicated that adding ethanol to the blend decreases combustion pressures, rate of heat release, smoke, and NO_x emission as well. The spray characteristics of blends of 2-methylfuran and gasoline were investigated by Wei *et al.* [12] using high speed Schlieren method. They demonstrated that the flash boiling is observed at low ambient pressures and decreasing the 2-methylfuran ratio of blend reduces the spray area and abates the flash boiling level. Sharma and Agarwal [13] studied the mixture mechanism for various injection pressures. They employed a gasoline DI injector and a high speed camera to investigate the spray microscopic properties. Phase Doppler interferometry has been applied to measure the droplet size and velocity. Moreover, SMD and probability density function have been taken into account and the results indicate that for the injection pressure of 200 bar gasoline fuel is the best. Ghahremani *et al.* [14] investigated the effects of ambient and injection conditions on spray behavior of several blends of gasoline and bio-ethanol fuels using a gasoline DI system. They studied macroscopic and microscopic characteristics of the spray experimentally and theoretically. Their results indicate that increasing the difference between injection and ambient pressures enhances the spray tip penetration while improves the atomization level of the spray. Applying air entrainment analysis, they reported that decreasing the bio-ethanol percentage of the blend increases the equivalence ratio and required air as well.

Spray behaviors and atomization level of bio-fuels and their influences on emissions and engine performance have been recently investigated [15, 16]. Based on the bio-ethanol fuel and in order to enhance the energy content of the fuel, modified bio-ethanol (MBE) with chemical formulation of $C_{11}H_{24}OH$ has been produced in the present work. In comparison with conventional fuels, the key advantages of MBE fuel as a new compound fuel are its long-chain HC, higher octane number, and oxygen content, and lower emissions. This paper presents spray characteristics of the MBE fuel as well as gasoline fuel applying high-speed visualization techniques. A graphical interface software is developed in this work, namely image analyzer pro (IAP) to analyze the images and extract the results. As Martin *et al.* [2] and Liu *et al.* [4] showed, ambient pressure significantly affects the spray development while ambient temperature has no important effect on it. In this respect in the present study, the influences of injection and ambient pressures on the spray of several blends of MBE and gasoline have been investigated. Pure gasoline fuel is designated as MBE0. MBE20 contains 20% of MBE fuel and gasoline fuel for the remaining part. The MBE100 indicates pure MBE fuel. Both macroscopic and microscopic behaviors of the injected spray such as spray tip penetration, cone angle, projected area, SMD, Ohnesorge number, and equivalence ratio have been studied and reported as well. Furthermore, considering atomization physics of the spray a new non-dimensional number, atomization index (AI), has been developed which determines the spray atomization level. Moreover, applying uncertainty analysis, the maximum uncertainty of theoretical part of the present work has been explored. Employing least squares method and curve fitting, some correlations are extracted and reported to model the experimental results.

Experimental set-up

Direct injection system

The DI system includes fuel tank, filter, high pressure pump, pressure gauge, regulator, common rail, single-hole injector, and combustion chamber as shown in fig. 1. The combustion chamber which is fabricated in this research is modeled and analyzed in ANSYS software for safety reasons. The external view of the chamber is a cube with dimensions of 120 × 120 × 163 mm. The internal view of that is a cylinder with diameter and length of 80 mm and 141 mm, respectively. Fuel flows from the fuel tank through the pump, regulator, and common rail to the injector and is injected into the visualized chamber. The interior is a single hole one with the radius of 0.15 mm, and the injection pressure is monitored using one 12 bit digital indicator and a pressure transmitter. Ambient temperature of the chamber is at room temperature and its pressure is adjusting by an air compressor between 1 and 5 bar. Injection pressure and its duration are controlled using an injector controller as well. Three different blends of MBE and gasoline fuels have been examined in this study. Table 1 illustrates the physical properties of these blends such as stoichiometric air fuel ratio, density, kinematic viscosity, and surface tension.

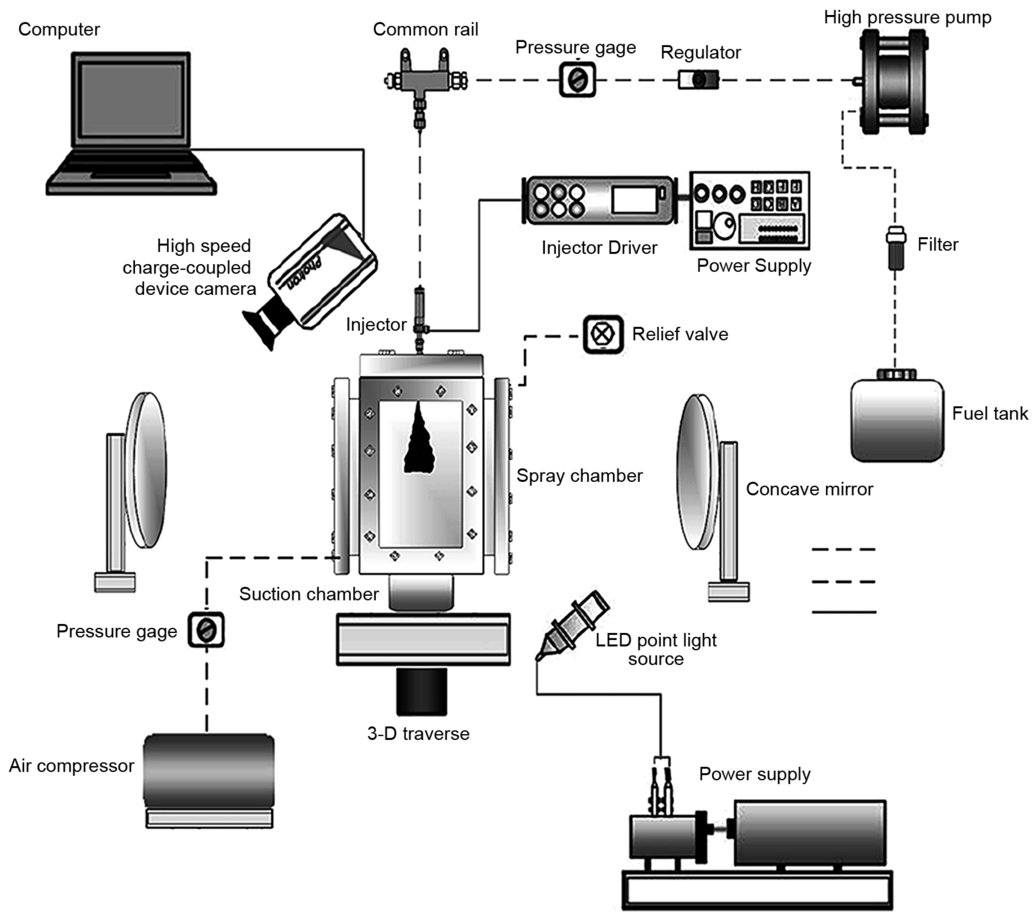

Figure 1. Schematic diagram of experimental test rig

Table 1. Physical properties of different tested blends

Fuel designation	Stoichiometric air-fuel ratio	Density [gcm^{-3}]	Kinematic viscosity [mm^2s^{-1}]	Surface tension [mNm^{-1}]
MBE0	15.10	0.749	0.64	18.680
MBE20	14.65	0.840	0.79	19.920
MBE100	13.33	0.873	1.79	24.535

Visualization and image analyzing systems

Imaging system contains one 1 W LED lamp, two parabolic mirrors with diameter of 90 mm, a high speed camera, a computer, and three optical windows with dimensions of 120 × 70 × 35 mm which are located around the combustion chamber. The present experiment employs a MotionBLITZ Cube3 as a high speed camera with imaging rate of up to 120,000 fps and maximum resolution of 512 × 512 pixels. Images which are recorded in the computer are analyzed by means of IAP. Figure 2 represents the graphical interface of the IAP software.

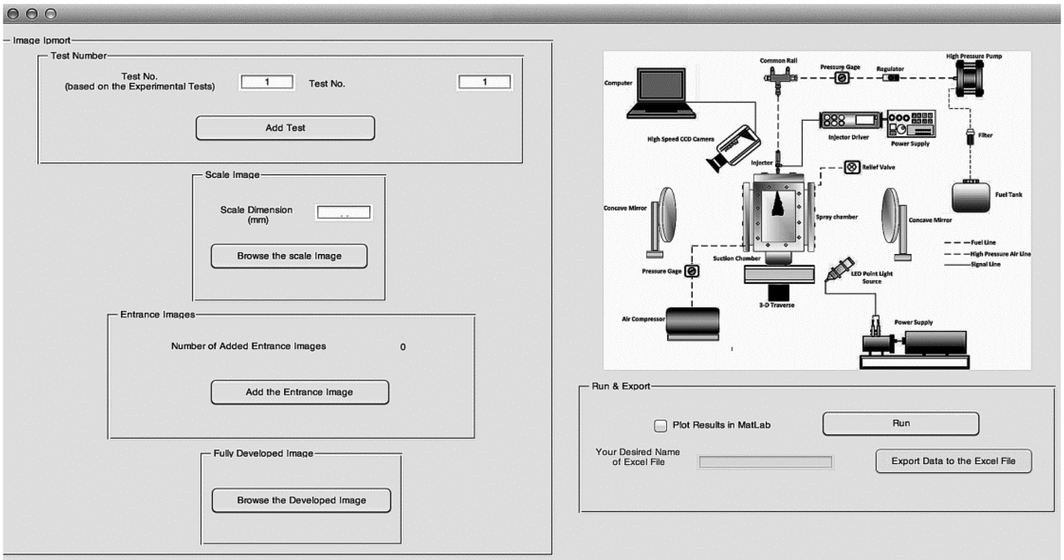

Figure 2. Graphical interface of IAP

The aforementioned software is developed user friendly and user should just browse the recorded images and click the run button, after that all images will be analyzed by IAP and the desired results could be reported graphically or exported in a Microsoft Excel file.

Spray geometry

The most important macroscopic characteristics of the spray are defined in fig. 3(a). The angle which is formed between injector exit and spray boundaries at 60 mm away from the injector exit hole, is defined as spray cone angle. Spray tip penetration length is defined as an axial distance between the farthest border of the spray and injector exit hole. As indicated in fig. 3(a), the hatched part of the spray image is defined as the spray projected area. Figure 3(b) shows a sample image of spray development which is recorded by experiment at injection pressure of 100 bar.

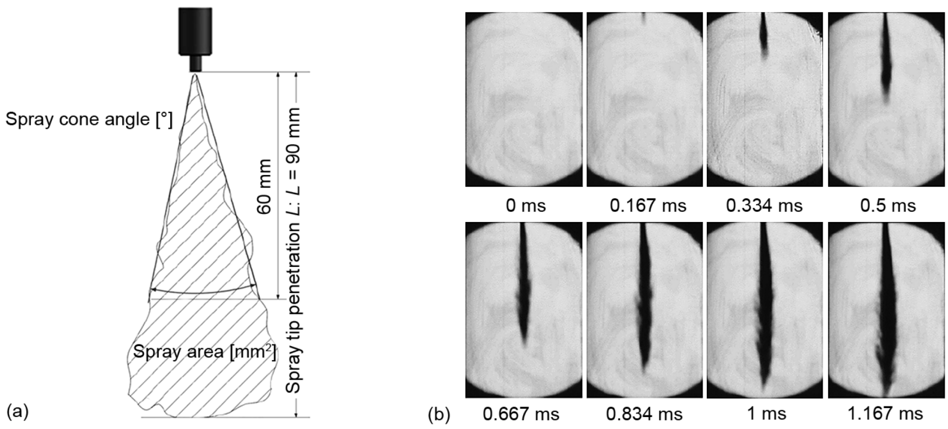

Figure 3. (a) Definition of macroscopic characteristics of spray, (b) A typical image of the spray evolution which is at 100 bar injection pressure

Table 2. Sensitivity of affecting parameters on the spray characteristics

Affecting parameter	Tip penetration length	Cone angle	Projected area
Injection pressure	2%	1.5%	3.5%
Ambient pressure	4%	3%	5%
Blend	5.5%	4.5%	6%
Knife edge position	3%	2%	4.5%

Sensitivity and error analysis

Kean [17] reported that Schlieren sensitivity is defined as a variation of illumination of the image in normal to knife edge distance. In this regard, in the present study the position of knife edge has been varied to visualize the images with the best quality. Moreover, the affecting parameters have been varied in the range of their measuring accuracy to investigate their effects on the spray characteristics. On the other hand, the process of recorded images is a direct method and the spray characteristics are obtained directly by analyzing the images, so the precision of the recorded images is one pixel. Table 2 shows the sensitivity analysis of the affecting parameters on the spray characteristics.

Moreover, to have an approximation of accuracy of the results, error analysis is performed. Equation (1) shows the general shape of the error analysis [18]:

$$\frac{U_Y}{Y} = \sqrt{\sum_{i=1}^{n} \left(\frac{1}{Y} \frac{\partial Y}{\partial X_i} U_{X_i} \right)^2} \tag{1}$$

where n is the number of dependent parameters, U_{Xi} – the X_i error, and U_Y – the error of parameter Y. Employing eq. (1), uncertainty of computed parameters could be reported.

Results and discussion

Spray cone angle

Since the spray cone angle is quite stable during the quasi-steady stage, in the present study, employing IAP software and analyzing the recorded images, average spray cone angle for various blends at different injection and ambient pressures is obtained and displayed in fig. 4. Ambient density acts as a virtual wall in front of the injected spray and increasing the ambient pressure increases the ambient density and aerodynamics drag force and resists the spray to go forward. Consequently spray will be propagated in radial direction and spray cone angle increases. Increasing the injection pressure enhances the spray momentum. It means that it helps the spray to overcome the aerodynamic drag force to penetrate axially, while the spray cone angle decreases. Adding MBE fuel in the blend reduces spray cone angle as a consequence of higher viscosity and surface tension of MBE compared with that of gasoline.

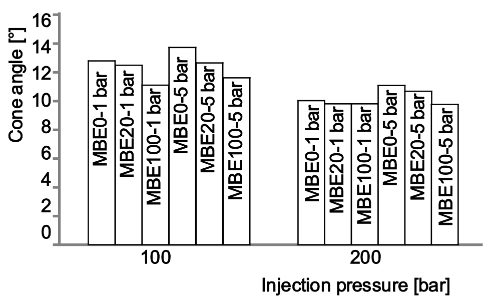

Figure 4. Average spray cone angle of different blends under multiple injection and ambient pressures

Spray tip penetration length

Figure 5 represents variation of spray tip penetration length *vs.* time for various blends of gasoline and MBE fuels which is obtained by analyzing the recorded images

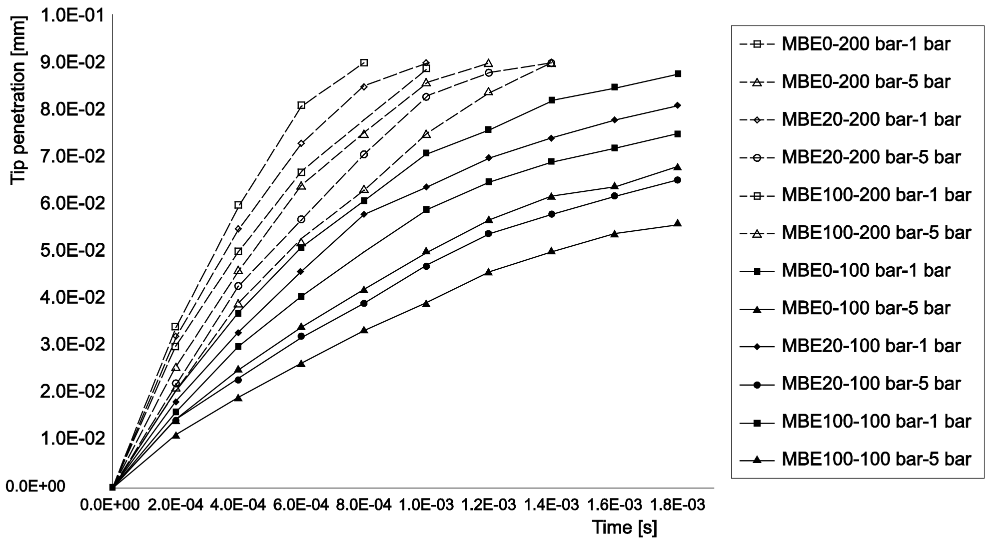

Figure 5. Spray tip penetration length *vs.* time for different blends at various injection and ambient pressures

by IAP software. Influences of injection and ambient pressures on tip penetration of all blends are indicated in this figure as well. As it is obvious in this figure the trend of all curves are the same with an increased deviation when time passes. Increasing the injection pressure enhances the spray momentum and let the spray to penetrate easily, so the spray tip penetration increases. Besides, Park *et al.* [19] based on the Roisman *et al.* [20] research divided the spray penetrating to the two key regions of main and front edge. They reported that in the main region the governing forces are the entrained ambient gas momentum and the injection inertia. Furthermore, the droplets inertia and the aerodynamic drag force are the governing forces in the front edge region. Moreover, results indicate the spray tip penetration decreases by increasing the ambient pressure due to enhancing the drag force. Adding MBE fuel to the blend increases tip penetration length due to higher viscosity, density, and surface tension of MBE fuel compared to those of gasoline.

Equation (2) represents a correlation for spray tip variation in time, which is extracted from experimental results employing least squares method. Applying this equation helps other researchers to predict and compare their results with experimental results of the present work with the maximum error of approximately 8%.

$$
\begin{gathered}
S = C_1(1 - \mathrm{e}^{-C_2 t}) \\
C_1 = 1.0 d^{-0.0001} \rho_\mathrm{f}^{-0.8071} \rho_\mathrm{a}^{-0.0168} \upsilon_\mathrm{f}^{-1.0761} \sigma_\mathrm{f}^{4.6608} (P_\mathrm{inj} - P_\mathrm{a})^{0.3820} \\
C_2 = 1.0 d^{-0.0001} \rho_\mathrm{f}^{0.4374} \rho_\mathrm{a}^{-0.2277} \upsilon_\mathrm{f}^{-2.9156} \sigma_\mathrm{f}^{11.5605} (P_\mathrm{inj} - P_\mathrm{a})^{0.5355}
\end{gathered} \tag{2}
$$

where S [m] is the tip penetration, C_1 and C_2 are constants which are calculated based on the related physical properties.

Spray projected area

Since the experimental results indicate that the spray shape is almost a regular cone with a little distortion, spray projected area could be considered as an acceptable approximation of the total injected fuel into the engine. By analyzing the images by means of IAP software, spray projected area has been computed and shown in fig. 6. Figure 6 indicates development of spray projected area *vs.* tip penetration length for different blends at various injection and ambient pressures. As expected the trend of all profiles are the same and increases by time. Regarding fig. 3(a), spray projected area is related to spray tip penetration length and cone angle directly. Increasing ambient pressure and decreasing injection pressure both increase spray projected area due to spray cone angle effect on the projected area. Figure 6 shows that adding MBE fuel in the blend almost decreases the spray projected area as well.

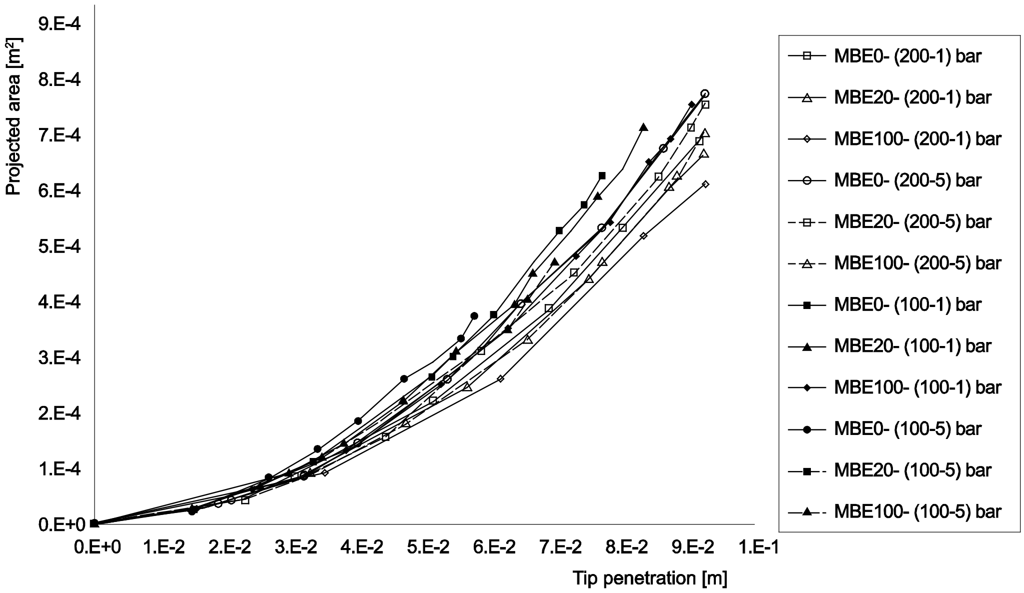

Figure 6. Variation of spray projected area *vs.* spray tip penetration length

Equation (3) is a correlation extracted from experimental results, which specifies development of spray projected area. Comparison of experimental results with those of obtained by eq. (3) demonstrates that error of using this correlation is less than 9%:

$$\begin{gathered} A = C_3 S^2 + C_4 S \\ C_3 = 1.0 d^{-0.0001} \rho_\mathrm{f}^{0.0222} \rho_\mathrm{a}^{0.0235} \upsilon_\mathrm{f}^{0.7071} \sigma_\mathrm{f}^{-3.0128} (P_\mathrm{inj} - P_\mathrm{a})^{-0.2674} \\ C_4 = 1.0 d^{-0.0001} \rho_\mathrm{f}^{-2.7697} \rho_\mathrm{a}^{0.4419} \upsilon_\mathrm{f}^{-12.8039} \sigma_\mathrm{f}^{45.0324} (P_\mathrm{inj} - P_\mathrm{a})^{0.3703} \end{gathered} \tag{3}$$

where A [m^2] is the spray projected area, S [m] – the spray tip penetration length, and C_3 and C_4 are constants in which could be calculated based on physical properties.

Air entrainment analysis

Sazhin *et al.* [21] reported that the quasi-steady jet theory is a well-developed hypothesis in this area, although these sprays are extremely transient which leads to the systematic discrepancies between experimental outcomes and theoretical predictions. Consequently, in the present study, applying quasi-steady jet theory, air entrainment analysis has been performed. Based on turbulent jet theory, Naber and Siebers [22], Desantes *et al.* [23], and Zhang *et al.* [24] explored air entrainment and developed eq. (4) for equivalence ratio [25]:

$$\phi(x,r) = 2.55\bar{\phi}(x)\mathrm{e}^{-\alpha\left(\frac{r}{R}\right)^2} \tag{4}$$

where $R = x\tan(\theta/2)$, and $\bar{\phi}(x)$ indicates the average equivalence ratio based on cross sectional area which is described in eq. (5):

$$\bar{\phi}(x) = \frac{2(AF)_{st}}{\sqrt{1+16\left(\frac{x}{x^*}\right)^2}-1} \tag{5}$$

where the characteristic length scale, x^*, is defined:

$$x^* = \frac{\sqrt{\rho_\mathrm{f} c_\mathrm{a}}\, d_\mathrm{o}}{0.75\sqrt{\rho_\mathrm{a}}\,\tan\left(\frac{\theta}{2}\right)} \tag{6}$$

where the value of 0.95 is suggested by Zhang *et al.* [24] for the orifice area contraction coefficient, c_a.

Regarding eqs. (3)-(5), equivalence ratio has a complicated behavior due to its dependency with several parameters such as physical properties of fuel and air, ambient and injection pressures, spray cone angle, and stoichiometric air-fuel ratio. Decreasing the stoichiometric air-fuel ratio of the blend and increasing the cone angle of the injected fuel both reduces equivalence ratio and required entrance air as well. Figures 7 and 8 display variation of equivalence ratio of the injected fuel in both axial and radial directions.

Development of equivalence ratio along axial direction and at $r = 0$ is demonstrated in fig. 7. Results reveal that equivalence ratio increases by decreasing the ambient pressure and enhancing the injection pressure, as a result of reducing the spray cone angle. Moreover, this figure demonstrates that increasing MBE percentage of the blend increases the ratio due to enhancing the density of the blend.

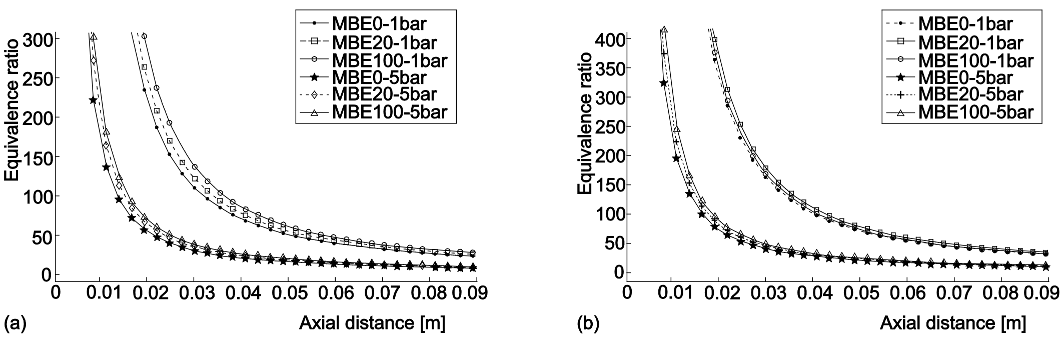

Figure 7. Equivalence ratio variation along central axial axis for different blends: (a) P_inj = 100 bar, (b) P_inj = 200 bar

Figure 8 illustrates radial development of equivalence ratio at x = 90 mm. Results indicate that equivalence ratio decreases by increasing ambient pressure, so the required air entrance is reduced. Profile shape of the equivalence ratio widens when ambient pressure increases as a consequence of increasing ambient density. Equivalence ratio decreases by reducing the injection pressure because of increasing the spray cone angle. Figure 8 demonstrates that at the peak of profile the highest variation of equivalence ratio is occurred. Besides, results indicate that equivalence ratio of pure gasoline fuel has the lowest and widest profile at a specific ambient and injection conditions and increasing the MBE fuel percentage of the blend increases the equivalence ratio due to increasing the blend density.

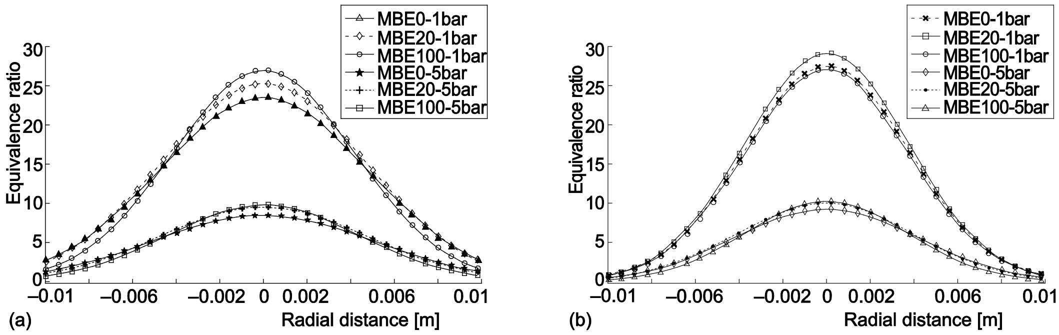

Figure 8. Radial development of equivalence ratio for different blends: (a) P_{inj} = 100 bar, (b) P_{inj} = 200 bar

Atomization index

Considering spray atomization physics, dimensional analysis has been performed to develop a new non-dimensional number, namely AI. This number determines the atomization level of the spray. The higher AI number indicates the higher atomization level and lower SMD. The AI number which is defined in eq. (7) is a function of physical properties of spray:

$$\text{AI} = \frac{\rho^2 U^3 d^2}{\mu \sigma} \tag{7}$$

Equation (7) illustrates that AI number is proportional to the ratio of square of inertia forces to product of viscous and surface tension forces. Considering measuring accuracy of different parameters of eq. (7) and applying eq. (1), error analysis verifies that uncertainty of AI number is less than 5.5%, as well.

Figure 9 shows variation of SMD of different blends and conditions with AI number. Ashgriz [26] and Ejim *et al.* [27] reported that SMD decreases while viscosity and surface tension of fluid decrease or density and velocity increase. Figure 9 verifies the mentioned findings.

One may realize that increasing the surface tension and viscosity of fuel increase SMD and prevent the droplet formation. Moreover, increasing the spray velocity due to increase in the difference between injection and ambient pressures reduces the SMD. Consequently, increasing injection pressure, decreasing ambient pressure, and using the fuel with lower viscosity and surface tension, all improve the atomization level of the spray. Since the physical properties of pure MBE are higher than those of gasoline fuel, adding MBE fuel to the blend decreases both AI number and atomization level. Besides, results indicate that pure gasoline fuel has the lowest SMD among all blends because of lowest viscosity and surface tension among all other blends.

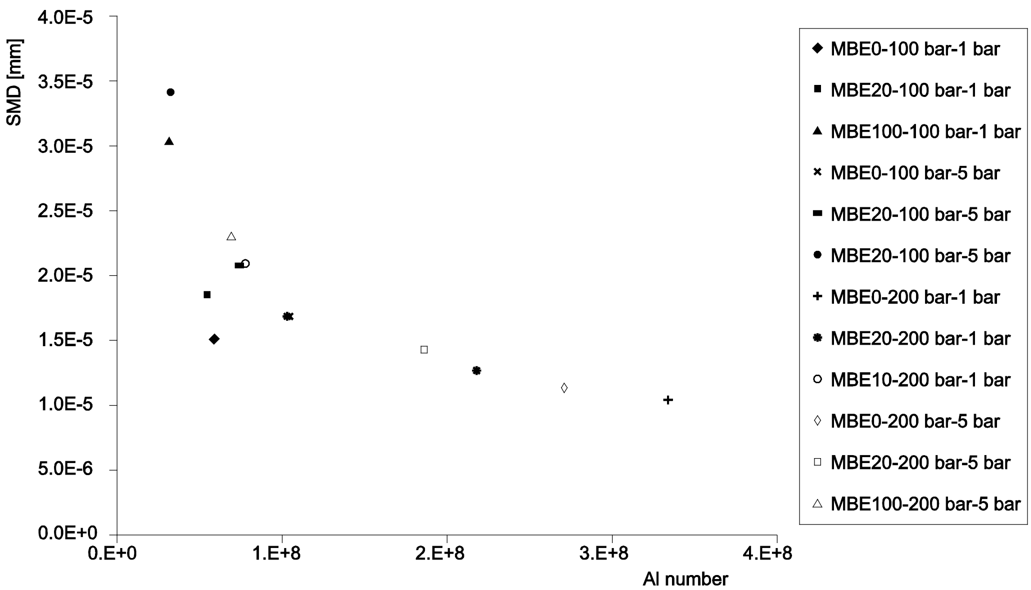

Figure 9. Variation of SMD *vs.* AI number for different blends conditions

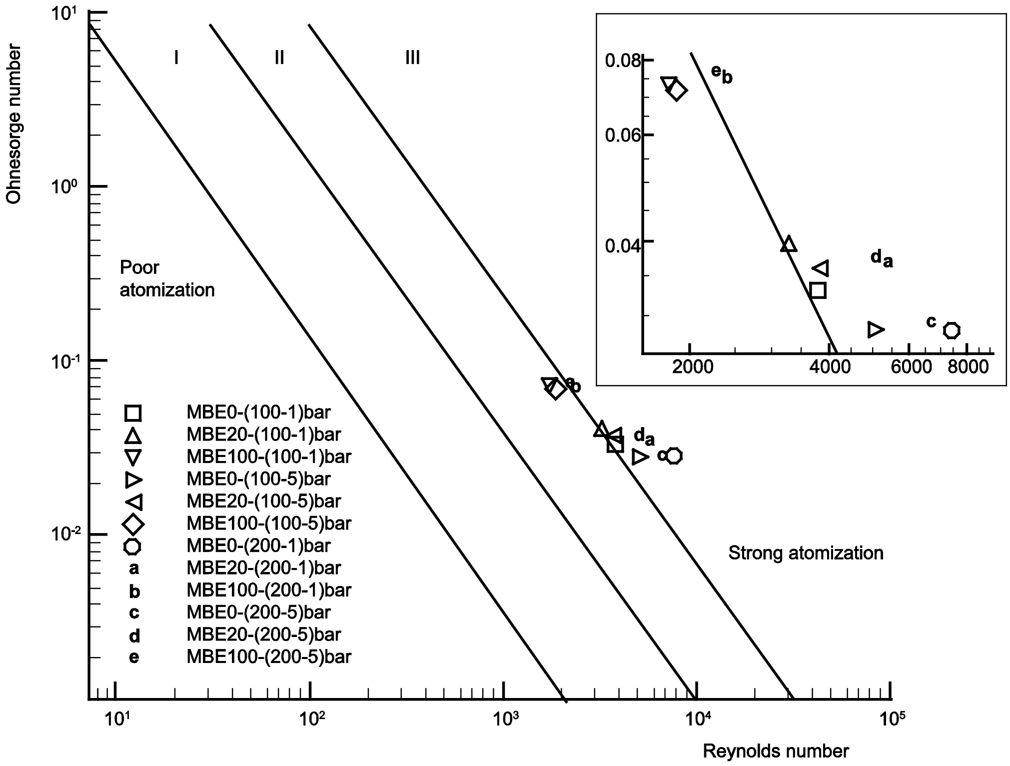

Figure 10. Variation of Ohnesorge number of different blends *vs.* Reynolds number under various injection and ambient conditions

Ohnesorge number

Ohnesorge number is a dimensionless number which is defined as the ratio of viscous force to the root square product of inertia and surface tension forces. The following equation describes this number:

$$\mathrm{Oh} = \frac{\mu}{\sqrt{\rho \sigma L}} \tag{8}$$

where L is the characteristic length scale.

Applying the error analysis based on the measuring accuracy of physical properties, specifies that the maximum error of applying eq. (8) for estimating the Ohnesorge number is about 4.3%. Wu *et al.* [1] divided the atomization level of the injected spray to three zones from strong atomization to poor atomization considering Ohnesorge number. Variation of Ohnesorge number *vs.* Reynolds number for different blends at various conditions is shown in fig. 10. Figure 10 shows that increasing both Ohnesorge and Reynolds numbers improves the atomization criteria. Increasing the injection pressure enhances the Reynolds number and progresses the atomization level of the spray as well. Since viscosity of the MBE fuel is higher than that of gasoline fuel, adding MBE fuel in the blends leads to the reduced Reynolds number although enhances the Ohnesorge number and retains the spray in the strong atomization zone.

Conclusions

In the present study macroscopic and microscopic properties of MBE fuel and its blends with gasoline fuel have been investigated experimentally and theoretically. Employing upgrading process of components of C10-C12 on the bio-ethanol fuel leads to produce a new alternative bio-fuel as a proper substitution for common fossil fuels in the gasoline DI engines. The most important advantages of the MBE fuel in comparison with gasoline fuel are higher oxygen content and octane number, lower emissions, and having the benefits of a long-chain HC fuel. Injection pressure, ambient pressure, and density have been varied to study their effects on three different blends of MBE and gasoline fuels. Macroscopic spray characteristics such as spray cone angle, spray tip penetration length, and spray projected area have been investigated and reported as well. Moreover, considering quasi-steady jet theory and atomization model, air entrainment analysis, mixture formation, and atomization behaviors of the spray have been studied. Furthermore, the present work introduces a new non-dimensional number namely AI to indicate the atomization level of spray. The concluding remarks are as follows.

- Decreasing injection pressure reduces spray tip penetration and equivalence ratio, though enhances spray cone angle, projected area, and SMD.
- Decreasing ambient pressure increases spray tip penetration and equivalence ratio, and decreases spray cone angle, projected area, and SMD.
- Raising gasoline percentage of the blend decreases spray tip penetration length, Ohnesorge number, and SMD, however increases Reynolds number and spray cone angle, due to lower physical properties of gasoline in comparison with MBE. Furthermore, results show that spray projected area increases by increasing the gasoline content of the blend.
- A new non-dimensional number, AI, which predicts the atomization level of the spray is developed and reported in the present study. Results show that the higher AI number leads to the lower SMD and improves the atomization level as well.

- Some correlations based on experimental results have been extracted and reported to allow other researchers to predict and compare their results with those of this work.
- Error analysis has been performed and the results reveal that the maximum error of computing AI and Ohnesorge numbers are 5.5% and 4.3%, respectively.

Nomenclature

A – spray area, [m^2]
$(AF)_{st}$ – stoichiometric air-fuel ratio, [–]
c_a – orifice area contraction coefficient, [–]
d – diameter, [m]
L – penetration length, [m]
Oh – Ohnesorge number, [–]
P – pressure, [bar]
r – radial distance, [m]
Re – Reynolds number (= Ud/υ), [–]
S – spray tip penetration, [m]
x – axial distance, [m]
x^* – characteristic length scale, [–]

Greek symbols

α – shape factor of Gaussian distribution, [–]
θ – spray cone angle, [–]
ρ – density, [kgm^{-3}]
σ – surface tension, [Nm^{-1}]
υ – viscosity, [ms^{-2}]
ϕ – equivalence ratio, [–]

Subscripts

a – ambient
f – fuel
inj – injection
o – orifice

References

[1] Wu, Z., *et al.*, An Experimental Study on the Spray Structure of Oxygenated Fuel Using Laser-Based Visualization and Particle Image Velocimetry, *Fuel*, *85* (2006), 10, pp. 1458-1464
[2] Martin, D., *et al.*, Investigation of the Influence of Multiple Gasoline Direct Injections on Macroscopic Spray Quantities at Different Boundary Conditions by Means of Visualization Techniques, *International Journal of Engine Research*, *11* (2010), 6, pp. 439-454
[3] Agarwal, A. K., *et al.*, Comparative Study of Macroscopic Spray Parameters and Fuel Atomization Behavior of Straight Vegetable Oils (Jatropha), Its Biodiesel and Blends, *Thermal Science*, *17* (2013), 1, pp. 217-232
[4] Liu, Y., *et al.*, A study of Spray Development and Combustion Propagation Processes of Spark-Ignited Direct Injection (SIDI) Compressed Natural Gas (CNG), *Mathematical and Computer Modelling*, *57* (2013), 1, pp. 228-244
[5] Kumar, G., Kumar, A., Spray Behavior Comparison in Diesel Engine with Biodiesel as Fuel, *Journal of Energy Technologies and Policy*, *3* (2013), 4, pp. 14-24
[6] Hiroyasu, H., Arai, M., Fuel Spray Penetration and Spray Angle in Diesel Engines, *Trans. JSAE*, *21* (1980), 5, pp. 11
[7] Pan, J., *et al.*, Spray and Combustion Visualization of Bio-Diesel in a Direct Injection Diesel Engine, *Thermal Science*, *17* (2013), 1, pp. 279-289
[8] Kim, K., *et al.*, Spray and Combustion Characteristics of Gasoline and Diesel in a Direct Injection Compression Ignition Engine, *Fuel*, *109* (2013), July, pp. 616-626
[9] Lee, S., Park, S., Experimental Study on Spray Break-up and Atomization Processes from GDI Injector Using High Injection Pressure Up to 30 MPa, *International Journal of Heat and Fluid Flow*, *45* (2014), Feb., pp. 14-22
[10] Wu, Z., *et al.*, Experimental Study on Spray Combustion Characteristics of Gasoline-Diesel Blended Fuel in a Controllable Active Thermo-Atmosphere, *Fuel*, *135* (2014), Nov., pp. 374-379
[11] Kim, Y., *et al.*, Effects of Ethanol Added Fuel on Exhaust Emissions and Combustion in a PCCI Diesel Engine, *Thermal Science*, *19* (2015), 6, pp. 1887-1896
[12] Wei, H., *et al.*, Experimental Analysis on Spray Development of 2-Methylfuran-Gasoline Blends Using Multi-Hole DI Injector, *Fuel*, *164* (2016), Jan., pp. 245-253
[13] Sharma, N., Agarwal, A. K., An Experimental Study of Microscopic Spray Characteristics of a GDI Injector Using Phase Doppler Interferometry, SAE technical paper, 2016-28-0006, 2016
[14] Ghahremani, A. R., *et al.*, Experimental and Theoretical Investigation on Spray Characteristics of Bio-ethanol Blends Using a Direct Injection System, *Scientia Iranica, Transaction B, Mechanical Engineering,* On-line first

[15] Chitsaz, I., *et al.*, Semi Analytical Solution to Transient Start of Weakly Underexpanded Turbulent Jet, *Journal of Fluids Engineering*, *133* (2011), 9, pp. 091204
[16] Chitsaz, I., *et al.*, Experimental and Numerical Investigation on the Jet Characteristics of Spark Ignition Direct Injection Gaseous Injector, *Applied Energy*, *105* (2013), May, pp. 8-16
[17] Kean, L., A Contribution to the Theory of Schlieren Sensitivity and Quantiative Evaluation, in, *DTIC Document*, Wright-Patterson Air Force Base, O., USA, 1962
[18] Mohammadi, M., *et al.*, Experimental Investigation of Thermal Resistance of a Ferrofluidic Closed-Loop Pulsating Heat Pipe, *Heat Transfer Engineering*, *35* (2014), 1, pp. 25-33
[19] Park, S. H., *et al.*, A Study on the Fuel Injection and Atomization Characteristics of Soybean Oil Methyl Ester (SME), *International Journal of Heat and Fluid Flow*, *30* (2009), 1, pp. 108-116
[20] Roisman, I. V., *et al.*, Effect of Ambient Pressure on Penetration of a Diesel Spray, *International Journal of Multiphase Flow*, *33* (2007), 8, pp. 904-920
[21] Sazhin, S., *et al.*, Jet and Vortex Ring-Like Structures in Internal Combustion Engines: Stability Analysis and Analytical Solutions, *Procedia IUTAM*, *8* (2013), pp. 196-204
[22] Naber, J. D., Siebers, D. L., Effects of Gas Density and Vaporization on Penetration and Dispersion of Diesel Sprays, SAE technical paper, 960034, 1996
[23] Desantes, J., *et al.*, Development and Validation of a Theoretical Model for Diesel Spray Penetration, *Fuel*, *85* (2006), 7, pp. 910-917
[24] Zhang, W., *et al.*, An Experimental Study on Flat-Wall-Impinging Spray of Microhole Nozzles under Ultra-high Injection Pressures, *Proceedings of the Institution of Mechanical Engineers, Part D: Journal of Automobile Engineering*, *222* (2008), 9, pp. 1731-1741
[25] Wang, X., *et al.*, Experimental and Analytical Study on Biodiesel and Diesel Spray Characteristics under Ultra-High Injection Pressure, *International Journal of Heat and Fluid Flow*, *31* (2010), 4, pp. 659-666
[26] Ashgriz, N., *Handbook of Atomization and Sprays: Theory and Applications*, Springer Science & Business Media, New York, USA, 2011
[27] Ejim, C., *et al.*, Analytical Study for Atomization of Biodiesels and their Blends in a Typical Injector: Surface Tension and Viscosity Effects, *Fuel*, *86* (2007), 10, pp. 1534-1544

Paper submitted: January 25, 2016
Paper revised: August 5, 2016
Paper accepted: August 23, 2016